



14<sup>th</sup> International Conference on Pressure Vessel Technology

## Experimental Investigation on the Kinetic Parameters of Diffusion Component for Vacuum Brazing SS316L/BNi-2/SS316L Joint

Z.P. Liu<sup>a</sup>, G.-Y. Zhou<sup>a,\*</sup>, F.Q. Tian<sup>a</sup>, D.Q. Chen<sup>a</sup>, S.-T. Tu<sup>a</sup>

<sup>a</sup>Key Laboratory of Pressure Systems and Safety (MOE), East China University of Science and Technology, Shanghai 200237, China

### Abstract

High temperature vacuum brazing has become the only appropriate process for thin-walled structures such as compact heat exchangers used in high-temperature gas-cooled reactor (HTGR) systems. During the typical brazing process, major attention should be paid to the isothermal solidification stage which has the most important influence on joint quality. However, the isothermal solidification process is controlled by the diffusion behavior of melting point depressant (MPD) elements, and only thorough diffusion of MPD elements into the base metal can result in the formation of the full solid-solution brazed joints. Therefore, it is significant for brazed joints to accurately obtain the kinetic parameters of diffusion component. In this study, a new type of wedge-shaped brazing specimen was proposed to study the joints properties. The experiments were carried out on the combination of SS316L with BNi-2 filler alloy at 1050, 1075 and 1100 °C with different holding time ranged from 15 to 45 min, respectively. Two classical models coupled with experimental data have been used to determine the kinetic parameters, including diffusion coefficient and diffusion activity energy. Then the effects of the brazing temperature and holding time on the maximum brazing clearance (MBC) value are also investigated. The results show that the diffusion coefficient increases with the increase of temperature and decreases with the increase of holding time at constant temperature. The diffusion activity energy of boron in SS316L is 134 kJ/mol. Meanwhile, significant augment of the MBC value has also been observed with increase in brazing temperature and holding time.

© 2015 The Authors. Published by Elsevier Ltd. This is an open access article under the CC BY-NC-ND license (<http://creativecommons.org/licenses/by-nc-nd/4.0/>).

Peer-review under responsibility of the organizing committee of ICPVT-14

**Keywords:** 316L Stainless Steel; Maximum brazing clearance; Wedge-shaped specimen; Diffusion coefficient ; Diffusion activity energy

\* Corresponding author. Tel.: + 86-021-64253513; fax: + 86-021-64253513  
E-mail address: [zhougy@ecust.edu.cn](mailto:zhougy@ecust.edu.cn).

## 1. Introduction

With the crisis of the world's energy, compact plate-fin structures have been widely used in many modern high-tech industry fields, such as the gas-turbine power generation systems, the hydrogen production systems, and high-temperature gas-cooled reactor (HTGR) [1-2]. These advanced thin-walled structures are used to improve the efficiency of the whole systems [3] and play a critical role in these high-tech systems. In order to obtain the high efficiency as possible, the operating temperature and pressure of the corresponding systems are higher and higher. Meanwhile, all devices in the systems tend to be miniaturized and microminiaturized. Accordingly, as one of typical components, it is much meaningful to study the manufacture technology and mechanical properties of these plate-fin structures. Since the conventional fusion welding and other welding methods are not appropriate for the microminiaturized structures, brazing has been used extensively to create attachments between metallic structures [4]. This process eliminates the need for a high bonding force due to the formation of a thin liquid interlayer, which differs from diffusion bonding. Especially for compact heat exchangers, vacuum brazing is the only cost-effective process that results in thousands of the most perfect joints between the fins and the primary surfaces [5].

During the typical high temperature brazing process, a low melting filler alloy containing melting point depressant (MPD) elements such as B is placed between faying surfaces of the base alloy and then the entire assembly is heated to the bonding temperature. Similar with transient liquid phase bonding, alternatively termed as diffusion brazing [6], brazing bonding process can be classified into a number of sequential discrete stages, namely, i) melting of the filler metal, ii) dissolution of the base metal, iii) isothermal solidification and iv) homogenization [7]. At the brazing joint area, diffusion of MPD elements induce a continuous modification of the liquid interlayer composition, which increases the melting temperature of the brazing seam area and results in re-solidification during holding stage at a constant brazing temperature. This mode of solidification is generally referred to as isothermal solidification to make a distinction from the usual case of solidification during cooling stage [8]. Major attention need to be paid to the isothermal solidification stage, because complete isothermal solidification can realize the full diffusion of MPD element into the base metal and finally form the full solid-solution joint. Otherwise, the brittle intermetallic compounds will be formed in the brazing seam due to insufficiently diffused MPD elements, which will lead to cracks near them and the significant reduction in structural strength and toughness [9-11]. However, the behaviour of diffusion component which is closely related to the formation of brittle phase is sensitive to the brazing parameters, such as brazing temperature, holding time and brazing clearance. In view of this, the experimental study based on wedge-shaped gap specimen could be a desirable approach to study the brazed joints. In the wedge-shaped gap joint, a distinction is made between areas free of brittle phase and brittle phase containing seam sections [12]. The initial formation of brittle phase stabilization marks the maximum brazing clearance (MBC) at brazed joint, where the diffusion components have been just completely diffused. Thus, the corresponding brazing time can represent the isothermal solidification time for that MBC.

The most ideal material of compact heat exchangers used in HTGR is SS316L, because of its good features such as excellent elevated temperature strength and remarkable corrosion resistance [13]. Considering the potential increasing engineering application of the stainless steel brazing technology in many industries, several stainless steel brazed joints have been investigated [12, 14, 15]. However, the experimental investigation of SS316L brazed joints based on wedged-shaped gap specimen, could be seldom found in the literature. The kinetic parameters of diffusion component were also not acquired, which would be beneficial to understand the diffusion mechanism of MPD elements in the future research. Additionally, the wettability of nickel-based BNi-2 filler alloy on stainless steels during bonding process is excellent, and also, alloying elements dissolved from the base metals efficiently interact with the nickel filler metal [16]. Therefore, SS316L and BNi-2 were chosen as the base metal and filler alloy for the current study, respectively.

In the present paper, in order to obtain the corresponding MBC values under specified brazing parameters, a new wedge-shaped specimen was designed and manufactured. Nine SS316L/BNi-2/SS316L joints were brazed and experimented at 1050, 1075 and 1100 °C with different holding time ranged from 15 to 45 min, respectively. Coupled with two classical models, the maximum brazing clearances under different process parameters and the kinetic parameters, including diffusion coefficient and diffusion activity energy, were determined. Then the effects of the brazing temperature and holding time on the MBC value were also investigated.

## 2. Experimental details

### 2.1. Materials and the wedge-shaped specimen

A commercial 316L austenitic stainless steel sheet and an amorphous BNi-2 foil were used as the base alloy and filler metal, respectively. Table 1 shows their actually measured chemical compositions in weight percent. Due to the chemical compositions of BNi-2 filler alloy is almost identical to the nominal compositions of it [16, 17], it can be reasonably confirmed that the melting temperature range for BNi-2 filler alloy is consistent with the nominal value.

Table 1. Chemical compositions of SS316L base metal and BNi-2 filler alloy

Material	Chemical compositions (wt.%)	Solidus (°C)	Liquidus (°C)
SS316L	C:0.57, Si:0.44, P:0.04, S:0.02, Mn:1.32, Ni:9.45, Cr:17.85, Mo:2.23, Fe: 68.09	--	--
BNi-2	B:4.92, C:0.76, Si:4.74, Cr:7.63, Fe:3.03, Ni:78.92	971	999

According to the Fig. 1a, the new wedge-shaped specimen is designed and manufactured to form a wedge-shaped groove, which can be considered as a variable joint clearance. This specimen consists of upper and lower portions, and both of them are SS316L. The width of upper portion (25 mm) is as wide as the width of the amorphous BNi-2 foil. The length of upper portion is 50 mm, and the selection of this value has a great impact on the formation of wedge-shaped groove. The size of the lower portion was designed to match the upper portion. The size of the wedge-shaped groove varies from 0 to 800  $\mu\text{m}$  approximately (Fig. 1b). The angle between the upper and lower portions is  $2.86^\circ$ . Ideally, the angle should be smaller, but it is limited by the machining accuracy actually. In addition, it should be also noted that for the new wedge-shaped specimen, the leakage of the molten filler alloy in the wedge groove due to extrusion or surface wetting and the convenience of experimental operation have been taken into account.

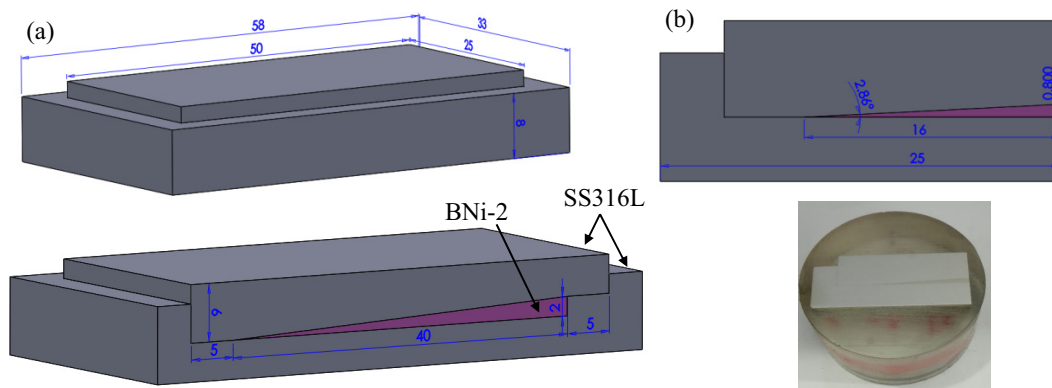


Fig. 1. (a) The schematic of the new wedge-shape specimen (mm); (b) the wedge-shaped joint (mm).

### 2.2. Experimental procedures

Prior to brazing operation, the faying surfaces of the base metal and filler alloy were ultrasonically degreased in acetone for 15 min. Adequate foils with 40  $\mu\text{m}$  in thickness were placed in the groove. Thereafter, the assembled specimen was entirely placed in a vacuum furnace with a heavy molybdenum lump on it to prevent it from moving.

According to Ou et al. [17] on the wetting angle measurements of BNi-2 filler alloy, it was observed that the molten BNi-2 filler alloy cannot get effectively wetting property at 1025  $^\circ\text{C}$ . Thus, the brazing parameters matrix in

current study was selected as shown in Table 2. The vacuum brazing heating cycle (Fig. 2) included the following parts: pumping the furnace to 0.007 Pa (step 1), heating at temperature from 20 to 850 °C within 50 min (step 2), holding at 850 °C for 30 min (step 3), and then heating to the brazing temperature within 40 min approximately (step 4), subsequent to this, holding stage within a preset time (step 5). After the completion of holding stage, the specimen was self-cooling in vacuum furnace (step 6).

Table 2. Brazing parameters matrix

Temperature (°C)	Holding time (min)		
1050	15	30	45
1075	15	30	45
1100	15	30	45

The bonded samples for metallographic investigation were sectioned from the brazed joints using a NC wire cut electro-discharge machine (WEDM), as shown in Fig. 1b. Thereafter, they were grinded, polished, etched in order and examined using the optical metallography and scanning electron microscope (SEM) equipped with electron dispersive spectrometry (EDS). Hardness values at the brazing seam were also measured by using a HXD-1000TMC/LCD hardness tester with a load of 100 gf.

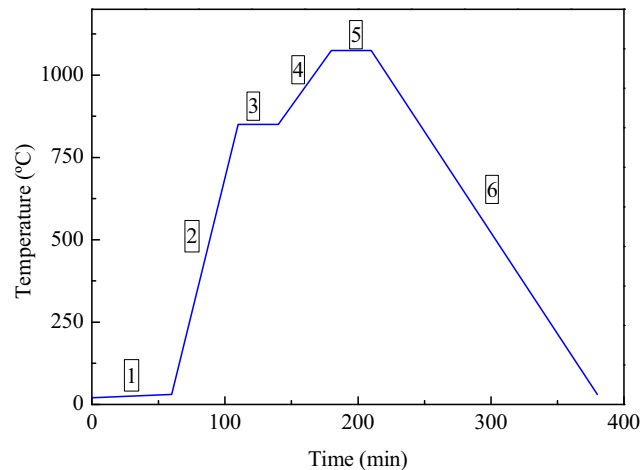


Fig. 2. The temperature history of vacuum brazing.

### 3. Diffusion based theories of kinetic parameters

#### 3.1. The acquisition approach of diffusion coefficient

The diffusion coefficient is a basic kinetic parameter of the atomic diffusion at joint interface. Compared with the joint formation mechanism of Transient liquid phase bonding (TLP), experimental researches of brazed joint microstructure with narrow gap identically tend to focus on the MPD elements diffusion behaviour of the filler alloy. Hence, analytical TLP models have been proposed to describe the kinetics process of the brazing in current study [18]. Several analytical TLP models have been proposed to describe the kinetics of the bonding process [19-23]. Almost of them can be classified into three types, namely, stationary solid/liquid interface model, solute distribution law model and migrating solid/liquid interface model, generally limited to a description of isothermal solidification stage. This assumes that there has been no solute prior diffusion on other stages such as dissolution, or widening, since dissolution of the solid phase and widening of the liquid layer normally occur within a very short time.

Zhou [23] examined the derivation procedures of the stationary solid/liquid interface model and migrating solid/liquid interface model to study the difference between them. It may be postulated that the stationary solid/liquid interface model got less accurate, migrating solid/liquid interface model provides a better approximation to simulate the process for the isothermal solidification stage. Correspondingly, Arafin et al. [22] indicated that although this solute distribution law model can be used for a reasonable approximation of isothermal solidification stage, the migrating solid/liquid interface model should be used for better accuracy and reliability. Therefore, in this paper, according to the comprehensive comparison of the above, the diffusion coefficient of boron component which is the major diffusion component in current study was determined by using the migrating solid/liquid interface model.

The migration of the solid/liquid interface is controlled by the diffusion of the boron component into the solid phase, driven by concentration gradient. Moreover, the solute conservation requirement in the solid makes it possible to apply the Fick's second law for the case of unidirectional diffusion [19]:

$$\frac{\partial C}{\partial t} = D \frac{\partial^2 C}{\partial x^2} \quad (1)$$

where  $C$  denotes the concentration of the boron component in the solid phase,  $D$  is the diffusion coefficient in the base metal, which is considered as a constant in this paper.

A general error function solution for the Fick's second law is used to calculate the concentration of the solute atom in the solid phase [21].

$$C(x, t) = A + B \operatorname{erf}\left(\frac{x}{2\sqrt{Dt}}\right) \quad (2)$$

where  $A$  and  $B$  are constants that determined by the specific boundary conditions. when  $x \rightarrow \infty$

$$C(\infty, t) = A + B = C_0 \quad (3)$$

and  $C_0$  is the initial solute concentration in the base metal. And at the moving solid/liquid interface  $x=x_s$

$$C(x_s, t) = A + B \operatorname{erf}\left(\frac{x_s}{2\sqrt{Dt}}\right) = C_s \quad (4)$$

where  $C_s$  is the solute concentration of the solid phase at the solid/liquid interface.

Since the Equation (4) will obey all values of  $t$ ,  $x_s$  must be proportional to  $t^{1/2}$ ,

$$x_s = \beta \sqrt{4Dt} \quad (5)$$

where  $\beta$  is a dimensionless constant. The mass balance at the solid/liquid interface satisfies the following relationship :

$$(C_L - C_s) \frac{dx_s}{dt} = D \left( \frac{\partial C(x, t)}{\partial x} \right)_{x=x_s} \quad (6)$$

where  $C_L$  is the solute concentration of the liquid phase at the solid/liquid interface. And the solution for  $\beta$  is given by solving Equations (2-6) [21].

$$\frac{\beta(1 + \operatorname{erf} \beta)\sqrt{\pi}}{\exp(-\beta^2)} = \frac{C_s - C_0}{C_L - C_s} \quad (7)$$

Therefore, for a given ratio of  $(C_s - C_0)/(C_L - C_s)$  by referring the phase diagram, the value of  $\beta$  can be estimated numerically. After that, according to Equation (5), the diffusion coefficient of boron component during brazing process with the selected brazing parameters can be calculated using the following expression:

$$D = \frac{(2h)^2}{16\beta^2 t_{IS}} \quad (8)$$

where  $t_{IS}$  is the time of isothermal solidification stage, which corresponds to the holding time of the experiment.  $2h$  is the final maximum width of the molten zone, also termed as maximum brazing clearance (MBC) value of the brazed joints.

### 3.2. The acquisition approach of diffusion activation energy

Another basic kinetic parameter for the atomic diffusion at joint interface is diffusion activity energy. For an atomic diffusion mechanism, whatever it is, gap mechanism, exchange mechanism or space mechanism, it requires external energy to overcome the energy barrier, which can be called diffusion activation energy. The diffusion activation energy will be influenced by the concentration of diffusion component and the cohesion force between the diffusion component and the other components, and then diffusion coefficient changes along with it. The atomic diffusion coefficient is required to meet the Arrhenius equation [24], which regulates the relationship between the diffusion coefficient with the diffusion activation energy  $Q$  and the diffusion constant  $D_0$ .

The famous Arrhenius equation is expressed as [25],

$$D = D_0 e^{-Q/RT} \quad (9)$$

where  $D_0$  is the diffusion constant,  $Q$  is the diffusion activation energy,  $T$  is the absolute bonding temperature and  $R$  is the gas constant. Taking the logarithm of both sides of Equation (9), one can get the following relationship:

$$\ln D = \ln D_0 - \frac{Q}{R} \frac{1}{T} \quad (10)$$

Since the diffusion activation energy  $Q$  and diffusion constant  $D_0$  are temperature independent, and only related to the diffusion mechanism and the nature of materials, there should be a good linear relationship between  $\ln D$  and  $1/T$ . After determining diffusion coefficient values  $D$  experimentally at different temperatures from Equations (1-8), the corresponding values of  $\ln D$  along with  $1/T$  could be calculated by fitting the experimental data.

## 4. Results and discussions

### 4.1. Determination of MBC value for the SS 316L/BNi-2/SS316L brazed joint

In this section, the specimens brazed for 45 min at 1050 and 1075 °C, respectively, were chosen as examples to describe the determination method of MBC value in detail, these results are shown in Table 3 and Fig. 3.

Table 3. Center zone constituents, characteristic of the brazed joint.

Brazed zone	Chemical compositions (wt.%)	Microhardness (HV)	phase
zone 1	Si:4.80, Cr:7.90, Fe:5.63, Ni:81.67	377.78	Ni-rich solid solution
zone 2	B:18.74, Si:2.23, Cr:36.74, Fe:2.81,	607.16	Cr-rich boride
	Ni:39.47		Ni-rich boride
zone 3	Si:5.31, Cr:6.72, Fe:6.17, Ni:81.79	388.54	Ni-rich solid solution
zone 4	B:21.99, Si:0.73, Cr:57.71, Fe:2.30,	624.68	Cr-rich boride
	Ni:17.27		Ni-rich boride

The initial formation of brittle phase stabilization marks the maximum brazing clearance (MBC) for the combination of base metals and filler alloy [22]. In the present wedge gap joint, a distinction is made between areas free of brittle phase, namely the region with full solid solution phase, and intermetallic compound phases with the variation of joint gap, as shown in Fig. 3.

The SEM-EDS compositional analysis of the centre zone (Table 3) suggests the brittle phases could be nickel-rich and chromium-rich borides. Using the hardness tester, the microhardness is determined by mean values of 5 measurements taken at the joint on each zone. The results indicate that the hardness of the brittle phases (Cr-rich boride, Ni-rich boride) is much higher than that of the Ni-rich solid solution. Formation of such extremely hard product has been found to provide a preferential low resistance path for crack initiation and/or propagation, which results in significant reduction in the strength of the joints [15].

Therefore, through above comprehensive analysis process, the MBC value of brazed joint under specific brazing process parameters can be determined accurately. Additionally, Fig. 3 shows that the diffusion of MPD element into the base metal during complete isothermal solidification is mainly grain boundary diffusion.

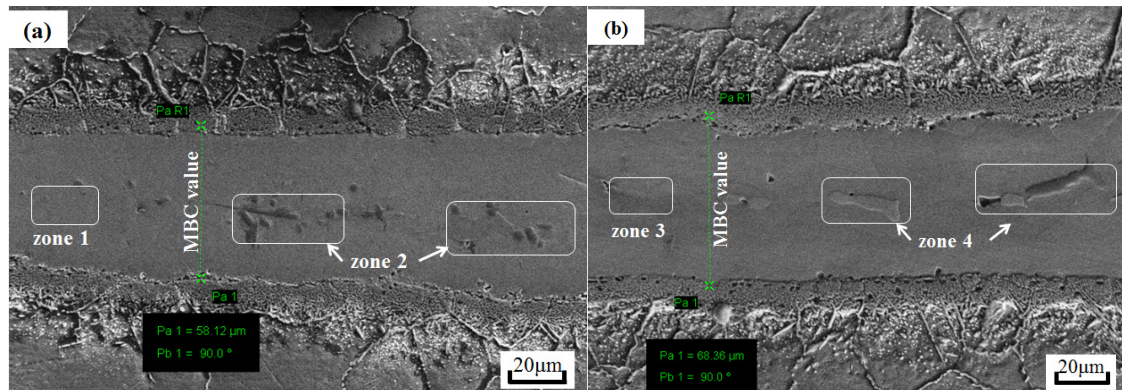


Fig. 3. SEM micrographs of SS316L/BNi-2/SS316L joint brazed at the holding time 45 min for a) 1050 °C and b) 1075 °C.

#### 4.2. Effects of the brazing temperature and holding time on the MBC

Figure 4 shows the whole MBC values for the SS316L/BNi-2 combination, brazed at 1050, 1075 and 1100 °C with different holding times ranged from 15 to 45 min, respectively. It is clear that, both the brazing temperature and the holding time have a strong influence on the MBC values, which are closely related to the kinetics behaviour of diffusion component during isothermal solidification stage. Significant augment of the MBC values has been observed with increase in brazing temperature and holding time. It is also found that the minimum MBC value is 39  $\mu\text{m}$ , which was acquired at 1050 °C within 15 min. Similarly, the maximum MBC value is 72  $\mu\text{m}$ , which was acquired at 1100 °C within 45 min.

However, in this section, that is not to say the higher the brazing parameters, the better the brazed joint. For high temperature brazing, the fusing dissolution of solid base metal in the molten liquid brazing filler alloy during brazing process is inevitable [26]. According to Arafin et al. [22], it was observed that the dissolution thicknesses of the base metal increased significantly with increasing bonding temperatures. Hence, if the dissolution process was not well controlled by optimizing the brazing process parameters, over-dissolution of base metal would result in corrosion holes in the thin-walled precision seal structures. The most appropriate brazing parameters for different thin-walled structures should be further investigated according to its industrial application.

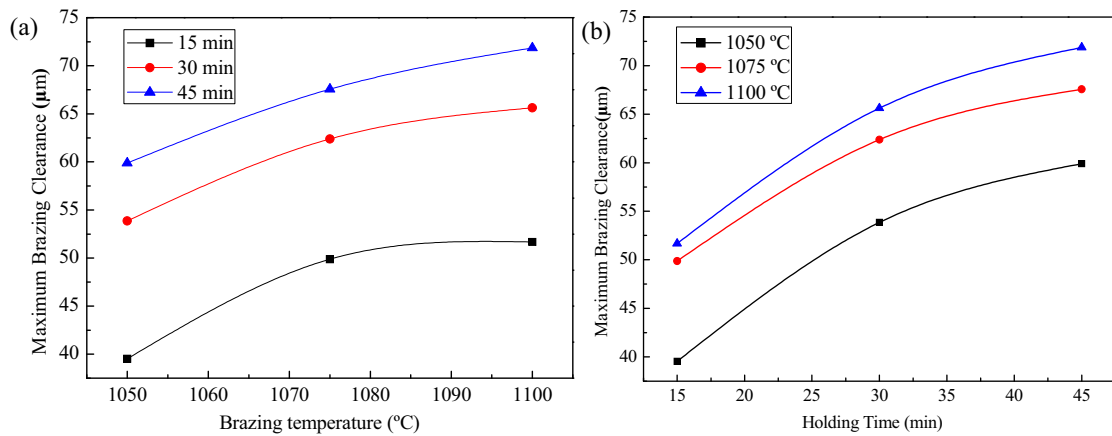


Fig. 4. Effects of the brazing temperature (a) and holding time (b) on the MBC.

#### 4.3. Calculation of diffusion coefficient for boron

The filler alloy BNi-2, which also can be described as multi-component Ni-Cr-B-Fe-Si interlayer, employs two melting point depressants (Si, B) with widely differing diffusion coefficients in the substrate material. The diffusion of B is essentially an interstitial atom in  $\gamma$ -Ni due to its small atomic size. Correspondingly, the diffusion coefficient of boron is four orders of magnitude higher than that of Si [15]. In addition, according to the Ni-Si, Ni-Cr and Ni-Fe phase diagram, the Ni can be mutually soluble with the Fe and Cr separately and dissolve an average of 15 at.% Si which is larger than actual concentration in the joint over the brazing temperature range. However, the boron limiting solubility in pure nickel is 0.3 at.% based on Ni-B binary phase diagram [14, 27]. Boron composition in joint centre area reached the solidus value during the holding stage due to the diffusion towards the base metal and thereafter, the formation of brittle phases was avoided during cooling.

Thus, it can be inferred that boron is the major solute element to form the intermetallic phases, only considering the kinetics parameters of boron for melting point depressants during diffusion-controlled isothermal solidification stage to be reasonable, and additionally, at the maximum brazing clearance (MBC) of brazed joint, the boron can all realize the thorough diffusion into the base metal.



To obtain the diffusion coefficients of boron in the base alloy at the three brazing temperatures, both Equations (1-8) and Fig. 4 need to be taken in to consideration. According to Arafin et al. [12], the assumption that the solubility limit of boron (0.3 at.%) in austenitic stainless steel 321, has been experimentally verified to be same with pure nickel or nickel-based alloys during TLP bonding with nickel-based filler alloy. Therefore, for the combination of austenitic stainless steel 316L and BNi-2 in current study,  $\beta$  in Equation (7) was calculated by taking  $C_s$  and  $C_L$  as the average solidus and liquidus boron composition of the present system, 0.3 and 16.6 at.%, respectively. The calculation values of diffusion coefficients are presented in Table 4.

Table 4. Diffusion coefficients of boron in SS316L.

Brazing temperature (°C)	Diffusion coefficients ( $\text{m}^2 \cdot \text{s}^{-1}$ ) $\times 10^{-10}$			
	15 min	30 min	45 min	mean
1050	10.31	9.57	7.89	9.25
1075	16.41	12.83	10.04	13.09
1100	17.62	14.20	11.36	14.39

In order to clearly study the effects of brazing temperature and holding time on diffusion coefficients of boron in SS316L, the values in Table 4 are plotted as shown in Fig. 5. The diffusion coefficient increases with the increase of temperature and decreases with the increase of holding time at a specific temperature. Ideally, the diffusion coefficient of solute atoms at a specified bonding temperature is constant. However, actually, for the diffusion-controlled isothermal solidification stage of the brazed joint, boron concentration gradient which is the main driving force of diffusion reduces gradually with the continuous diffusion of boron towards the base metal. Thus, Fig. 5 indicates the actual diffusion behaviour of the boron during isothermal solidification process.

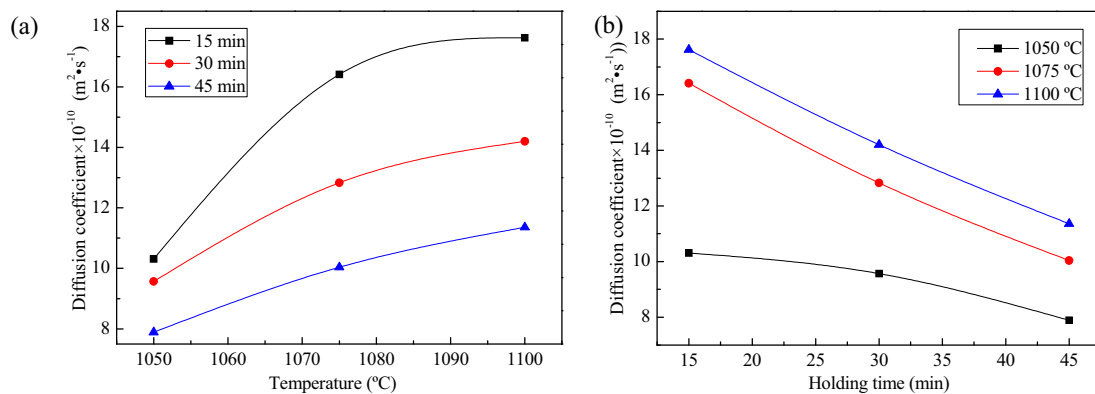


Fig. 5. Effects of brazing temperature (a) and holding time (b) on the diffusion coefficient of boron.

#### 4.4. Calculation of diffusion activity energy for boron

The obtained diffusion coefficients from Table 4 were then used in the empirical Equation (9) to calculate the diffusion activity energy of boron in SS316L. The logarithmic values of the diffusion coefficients ( $\ln D$ ) against the corresponding inverse temperature ( $1/T$ ) are plotted as shown in Fig. 6. The slope and intercept of the line are determined by fitting the data points.

In this study, the apparent activation energy  $Q$  for boron and its diffusion constant  $D_0$  in SS316L during isothermal solidification stage were computed to be 134 kJ/mol and  $0.000187 \text{ m}^2/\text{s}$ . Meanwhile, as shown in Table 5, through summarizing the investigation of other researchers on diffusion activation energy of boron in different materials [12, 22, 28, 29], it is observed that the diffusion activation energies of boron in conventional stainless

steels are smaller than those in pure nickel and nickel based alloys. Thus, compared with nickel based materials, the diffusion of boron atom in conventional stainless steels occurs much easier during isothermal solidification stage.

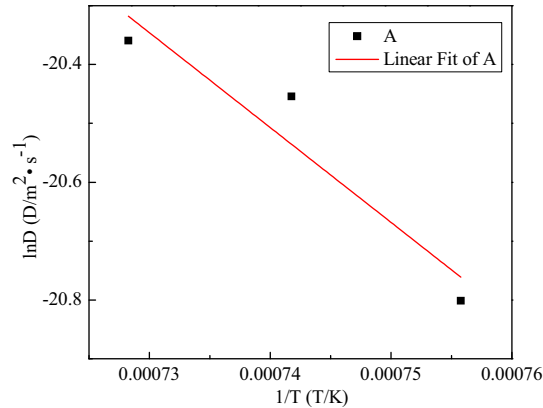


Fig. 6. The logarithmic values of diffusion coefficients ( $\ln D$ ) versus  $1/T$ .

Table 5. Diffusion activation energies of boron in different materials.

Material	Diffusion constant ( $\text{m}^2/\text{s}$ ) $\times 10^{-4}$	Diffusion activity energy (kJ/mol)
SS316L	1.87	134
SS410	0.36	120
SS321	1.57	136
inconel718	12230463	310
inconel625	34773.45	242
Inconel738	144	211
Ni	140	226

## 5. Conclusions

The wedge-shaped joint specimens of SS316L were prepared and experimentally brazed using BNi-2 filler alloy. Two classical analytical models of kinetic parameters coupled with experimental data have been used to study the kinetic parameters of diffusion component (boron). The following conclusions can be drawn:

- 1) A new type of wedge-shaped brazing specimen is designed and successfully employed to acquire the corresponding MBC values at 1050, 1075 and 1100 °C with different holding times ranged from 15 to 45 min, respectively. In this study, the MBC values at SS316L/BNi-2/316L joint are from 39 to 72  $\mu\text{m}$ .
- 2) Significant augment of the MBC value has been observed with increase in brazing temperature and holding time. Due to the fusing dissolution of solid base metal in the molten liquid brazing filler alloy, the most appropriate brazing parameters for different thin-walled structures should be further investigated according to its industrial application.
- 3) The diffusion coefficients of boron in SS316L were acquired by using migrating solid/liquid interface model coupled with experimental data. The diffusion coefficient of boron at a specified bonding temperature is not constant, and it increases with the increase of temperature and decreases with the increase of holding time.
- 4) The diffusion activation energy  $Q$  of boron in SS316L was computed to be 134 kJ/mol. Compared with pure nickel and nickel based alloys, the diffusion activation energies of boron in conventional stainless steels are much smaller.

## Acknowledgements

This research was sponsored by Shanghai Pujiang Program (No. 14PJD015).

## References

- [1] F. Kawashima, T. Igari, Y. Miyoshi, et al. High temperature strength and inelastic behavior of plate–fin structures for HTGR[J]. Nuclear engineering and design, 2007, 237(6): 591-599.
- [2] H. Chen, J.M. Gong, S.T. Tu, et al. Diffusion-Based Analytical Modeling of Brazing Stainless Steel with BNi-2[J]. Journal of Computational and Theoretical Nano science, 2008, 5(8): 1746-1752.
- [3] W.C. Jiang, J.M. Gong, S.T. Tu, et al. Modelling of temperature field and residual stress of vacuum brazing for stainless steel plate-fin structure[J]. Journal of materials processing technology, 2009, 209(2): 1105-1110.
- [4] S.T. Tu, G.Y. Zhou, X.H. Yu, Microminiaturization of chemo-mechanical system and energy conservation, Chemical Industry And Engineering Progress[J], 2007, 26(2): 253-261.
- [5] R.K. Shah, Advances in science and technology of compact heat exchangers[J]. Heat Transfer Engineering, 2006, 27(5): 3-22.
- [6] W.D. MacDonald, T.W. Eagar, Isothermal solidification kinetics of diffusion brazing[J]. Metallurgical and materials Transactions A, 1998, 29(1): 315-325.
- [7] W.D. MacDonald, T.W. Eagar, Transient liquid phase bonding[J]. Annual review of materials science, 1992, 22(1): 23-46.
- [8] W.F. Gale, D.A. Butts, Transient liquid phase bonding[J]. Science and Technology of Welding & Joining, 2004, 9(4): 283-300.
- [9] X.Q. Li, L. Li, K. Hu, et al. Vacuum brazing of TiAl-based intermetallic with Ti–Zr–Cu–Ni–Co amorphous alloy as filler metal[J]. Intermetallics, 2015, 57: 7-16.
- [10] A. Laik, A.A. Shirzadi, R. Tewari, et al. Microstructure and interfacial reactions during active metal brazing of stainless steel to titanium[J]. Metallurgical and Materials Transactions A, 2013, 44(5): 2212-2225.
- [11] N.R. Philips, C.G. Levi, A.G. Evans, Mechanisms of microstructure evolution in an austenitic stainless steel bond generated using a quaternary braze alloy[J]. Metallurgical and Materials Transactions A, 2008, 39(1): 142-149.
- [12] M.A. Arafin, M. Medraj, D.P. Turner, et al. Effect of alloying elements on the isothermal solidification during TLP bonding of SS 410 and SS 321 using a BNi-2 interlayer[J]. Materials Chemistry and Physics, 2007, 106(1): 109-119.
- [13] Z.L. An, W.L. Luan, F.Z. Xuan, et al. High temperature performance of 316L-SS joint produced by diffusion bonding[C]//Key Engineering Materials. 2005, 297: 2795-2799.
- [14] H. Chen, J.M. Gong, S.T. Tu, Numerical modeling and experimental investigation of diffusion brazing SS304/BNi-2/SS304 joint[J]. Science and Technology of Welding & Joining, 2009, 14(1): 32-41.
- [15] X.J. Yuan, C.Y. Kang, M.B. Kim, Microstructure and XRD analysis of brazing joint for duplex stainless steel using a Ni–Si–B filler metal[J]. Materials Characterization, 2009, 60(9): 923-931.
- [16] F.Z. Wang, Q.Z. Wang, B.H. Yu, et al. Interface structure and mechanical properties of Ti (C, N)-based cermet and 17-4PH stainless steel joint brazed with nickel-base filler metal BNi-2[J]. Journal of Materials Processing Technology, 2011, 211(11): 1804-1809.
- [17] C.L. Ou, D.W. Liaw, Y.C. Du, et al. Brazing of 422 stainless steel using the AWS classification BNi-2 Braze alloy[J]. Journal of materials science, 2006, 41(19): 6353-6361.
- [18] H. Chen, J.M. Gong, S.T. TU, et al. State-of-art in Simulation of Brazing Packaging for Miniaturized Multi-channel Heat Exchanger[J]. Chinese journal of mechanical engineering, 2008, 44(4): 1-9.
- [19] I. Tuah-Poku, M. Dollar, T.B. Massalski, A study of the transient liquid phase bonding process applied to a Ag/Cu/Ag sandwich joint[J]. Metallurgical and Materials Transactions A, 1988, 19(3): 675-686.
- [20] W.D. MacDonald, T.W. Eagar, Isothermal solidification kinetics of diffusion brazing[J]. Metallurgical and materials Transactions A, 1998, 29(1): 315-325.
- [21] Y. Zhou, W.F. Gale, T.H. North, Modelling of transient liquid phase bonding[J]. International Materials Reviews, 1995, 40(5): 181-196.
- [22] M.A. Arafin, M. Medraj, D.P. Turner, et al. Transient liquid phase bonding of Inconel 718 and Inconel 625 with BNi-2: Modeling and experimental investigations[J]. Materials Science and Engineering: A, 2007, 447(1): 125-133.
- [23] Y. Zhou, Analytical modeling of isothermal solidification during transient liquid phase (TLP) bonding[J]. Journal of materials science letters, 2001, 20(9): 841-844.
- [24] L.J. Karssemeijer, A. Pedersen, H. Jónsson, et al. Long-timescale simulations of diffusion in molecular solids[J]. Physical Chemistry Chemical Physics, 2012, 14(31): 10844-10852.
- [25] Y. Wu, X. Lu, S. Tong, Arrhenius relationship and two-step scheme in AF hyperdynamics simulation of diffusion of Mg/Zn interface-TNMSC[J]. The Chinese Journal of Nonferrous Metals, 2015, 23(2).
- [26] X.P. Zhang, Y.W. Shi, A dissolution model of base metal in liquid brazing filler metal during high temperature brazing[J]. Scripta materialia, 2004, 50(7): 1003-1006.
- [27] M. Pouranvari, A. Ekrami, A.H. Kokabi, Microstructure development during transient liquid phase bonding of GTD-111 nickel-based superalloy[J]. Journal of alloys and compounds, 2008, 461(1): 641-647.
- [28] O.A. Ojo, N.L. Richards, M.C. Chaturvedi, Isothermal solidification during transient liquid phase bonding of Inconel 738 superalloy[J]. Science and Technology of Welding & Joining, 2004, 9(6): 532-540.

- [29] Y. Nakao, K. Nishimoto, K. Shinozaki, et al. Analysis of isothermal solidification process on transient liquid insert metal diffusion bonding[J]. QJ Jpn. Weld. Soc, 1989, 7: 213-219.